RSC Mechanochemistry

ROYAL SOCIETY OF CHEMISTRY

PAPER

View Article Online
View Journal | View Issue

Cite this: *RSC Mechanochem.*, 2025, **2**, 756

Amplification of spiropyran mechanophore activation in bulk polymers through a tethering strategy†

Sanjit Narendran,[a] Zhenghao Zhai [a] and Yangju Lin *[ab]

Received 10th March 2025
Accepted 26th June 2025

DOI: 10.1039/d5mr00037h

rsc.li/RSCMechanochem

The insertion of force-active molecules (mechanophores) with optical-switching properties into polymer chains has enabled the development of various mechanochromic polymers. Among them, colorimetric spiropyran (SP) has been the most extensively studied. However, the low extent of SP activation in bulk materials and the associated poor material mechano-sensitivity have hindered its broader applications. To address this challenge, we report the amplification of SP mechanophore activation in bulk materials through a tethering design. Two SP mechanophores were tethered through a long aliphatic linker, and the resulting molecule was employed as a crosslinker in silicone elastomer networks. This approach resulted in an enhancement of SP activation by more than twofold compared to its mono-SP counterpart. Additionally, we observed that increasing the number of added short linkers leads to greater tension constraints on these linkers, creating a self-reinforcing effect on mechanophore activation. We anticipate that this tethering strategy can be adapted to other non-scissile mechanophores in bulk studies.

Introduction

Polymer materials are subjected to mechanical load during their lifespan, leading to aging and, eventually, failure of materials.[1,2] The disruption of their structural integrity is associated with the underlying stretching and scission of polymer strands at the molecular level. Early research primarily scrutinized the degradation behaviour of polymers under various types of mechanical loads, such as mastication,[3] flow shearing,[4] ultrasonication,[5] and extrusion,[6] with typically unselective chain/bond scissions observed. Initial attempts to harness mechanical force for selective bond scissions were demonstrated by solution studies of polymers embedded with weak peroxide[7] and azo[8] groups. The selective utilization of strained polymer strands in bulk materials was first reported by Sottos and coworkers, who incorporated a switchable spiropyran (SP) molecule into poly(methyl acrylate) and poly(-methyl methacrylate) matrices as a force probe.[9] They observed pronounced optical signals in the strained bulk materials resulting from the mechanical activation of the SP molecule.

Organic functional molecules covalently embedded within polymer backbones that selectively undergo transformations in response to mechanical force such as the aforementioned peroxide and azo compounds and SP, are termed mechanophores.[10] The judicious molecular designs[11,12] of mechanophores have enabled stress-responsive polymers exhibiting a wide range of functions, including altering optical signals,[13] releasing small-molecules,[14,15] catalysing reactions,[16,17] self-recovering/strengthening,[18] and on-demand degradation.[19]

Polymer materials that can sense mechanical load through switching optical signals (referred to as mechanochromic polymers) are particularly useful in indicating strained polymer strands,[20,21] force constraints,[22,23] and material overloads and damages.[21] These materials offer opportunities in understanding material fundamentals[24–27] and developing self-alarming materials[28] for potential facilitated repairing/replacing processes. SP has been the most extensively studied mechanophore that enables mechanochromic polymers.[29] When materials are subjected to mechanical load, mechanical force transduced to SP molecules preferentially cleaves the weak C–O bond, triggering a ring-opening reaction that converts the colourless SP form into the coloured merocyanine (MC) form (Fig. 1).

The intrinsic reactivity of the SP mechanophore can be tuned through substituent design,[30] regiochemical design[31] and choice of the polymer matrix.[32] However, the activation of SP mechanophores in stretched polymer networks remains relatively low,[33] which translates to a low material mechano-sensitivity. Theoretical modelling has indicated a force distribution in a stretched polymer network, with a low distribution probability of strands experiencing high forces (>100 pN).[34] Meanwhile, single molecule force spectroscopy (SMFS) revealed an activation force of 240–415 pN for some reactive SPs.[32,35] A

[a]*Department of Chemistry, University of Waterloo, Waterloo, Ontario N2L 3G1, Canada. E-mail: yangju.lin@uwaterloo.ca*

[b]*Waterloo Institute for Nanotechnology, University of Waterloo, Waterloo, Ontario N2L 3G1, Canada*

† Electronic supplementary information (ESI) available. See DOI: https://doi.org/10.1039/d5mr00037h

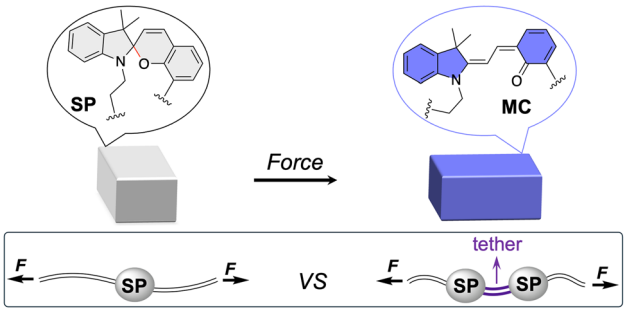

Fig. 1 Spiropyran-based mechanochromic polymer materials, and amplification of spiropyran activation in bulk materials through a tethering strategy.

similar result was observed for a *gem*-dichlorocyclopropane mechanophore derivative, which was activated at 900 pN in the SMFS study and exhibited only ~0.2% activation in polymer networks.[36] As such, unlike the mechanophore activation in plastic materials[37–40] or using other mechanical methods such as ball milling or grinding,[41,42] the historically low SP activation in stretched polymer networks seems to be intrinsic to both the mechanochemical reactivity of SP and the force-transduction limitations of polymer network matrices.

Strategies such as employing pre-swollen polymer matrices[43] or multi-network design[20,44,45] can enhance SP activation in stretched polymer networks. However, these polymer topology modifications either drastically alter material properties by introducing a plasticizer or create single-use materials by sacrificing the first network. Other strategies such as introducing crystalline polymer chains,[46] anchoring SP at the composite interface,[22] and concentrating SP as crosslinkers on the surface of different materials[47] can also improve mechanophore activation. Despite these advances, achieving a high extent of SP activation in stretched polymer networks remains challenging. We therefore aim to improve the SP activation in stretched polymer networks (*i.e.*, material mechano-sensitivity) by leveraging tension transduction along individual polymer chains for activation of tethered SP (**tSP**) mechanophores (Fig. 1). Unlike conventional single-SP systems, our approach positions two SP units to undergo simultaneous activation within a single chain or crosslinker. This strategy is hypothesized to amplify both mechanophore activation and material sensitivity compared to existing systems.

Results and discussion

Design of the tSP mechanophore

A previous study by De Bo *et al.*[48] investigated the mechanical reactivity of two tethered Diels–Alder adduct mechanophores. Despite the innovative tethered design, no substantial difference in reactivity was observed, likely due to the scissile nature of the mechanophores and the relatively long and flexible tethers employed. Additionally, the design of tethered mechanophores shares similarity with several bis-naphthopyran (BNP) mechanophores developed by Robb *et al.*,[49–51] which are fused structures containing short, rigid, and conjugated tethers. Interestingly, in these BSP mechanophores, the activation of one mechanophore appeared to influence the reactivity of the other. The non-equivalent reactivities of these two fused mechanophores can be attributed to electronic and/or geometry effects. Another notable study on bis-rhodamine mechanophores by De Bo, Cao and Chen *et al.*,[52] reported enhanced mechanochemical reactivity compared to the mono-counterpart. This improved reactivity was further attributed to a cooperative effect arising from both geometry and electronic factors.

To rule out interactive effects between the two tethered SPs, we chose a long aliphatic linker with ten carbon atoms to ensure that both SPs exhibit identical mechanical reactivity. As shown in Scheme 1, 1,10-dibromodecane was first reacted with 2,3,3′-trimethyl indolenine to produce a bis-indolenium salt **1**. Subsequent condensation of **1** with 2,3-dihydroxybenzaldehyde yielded a tethered SP diol molecule **2**, which was further functionalized with diene to provide the final compound **tSP**. For comparison, we also synthesized a mono-SP diene (**SP**) and a control diene (**Ctl**). The installation of the diene functionality allows these compounds to serve as crosslinkers in polydimethylsiloxane (PDMS) elastomer networks prepared using the commercial Sylgard 184 kit.[53] To ensure clarity in comparison, the contour lengths of all synthesized crosslinkers were kept similar. Previous studies have demonstrated that within a wide range of Kuhn numbers (1.1–5.7; contour length of 14.3–74.1 Å; Kuhn length = 13 Å for PDMS), the linker length has a negligible effect on the relative activation due to the non-affine deformation of strands.[54] Therefore, minor variances in the crosslinker length are unlikely to contribute to the activation difference.

Formulation of elastomer networks

We used the commercial Sylgard 184 kit to incorporate mechanophores into PDMS elastomer networks (Fig. 2). The feasibility of inserting diene-containing molecules through the platinum-catalysed hydrosilylation reaction is well-established in previous studies.[31,53,55,56] We incorporated the **tSP** mechanophore into the PDMS elastomer at 0.5 wt% relative to the material, with a base/curing reagent ratio of 10 : 1. To comprehensively assess the relative activation of the **tSP** mechanophore and the corresponding material mechano-sensitivity, we fabricated four additional sets of samples. Formulation details for all PDMS elastomer networks are provided in Table 1. Specifically, the molar number of the **tSP** mechanophore linker ($n = 5.8 \times 10^{-6}$ mol per gram elastomer) was used as a reference, and other linkers with the corresponding molar number were added accordingly. For example, the molar number of added linkers in **N(SP)** equals that in **N(tSP)**, while it is twice that in **N(2SP)**, **N(Ctl+tSP)**, and **N(2tSP)**. Notably, **N(Ctrl+tSP)** contains equal molar amounts of **Ctl** and **tSP** linkers.

For all elastomer networks, the amount of added diene linker was less than 2.2 mol% or 4.4 mol% relative to the PDMS base (vinyl-terminated PDMS linker), ensuring that the mechanical properties of the resulting PDMS elastomers were

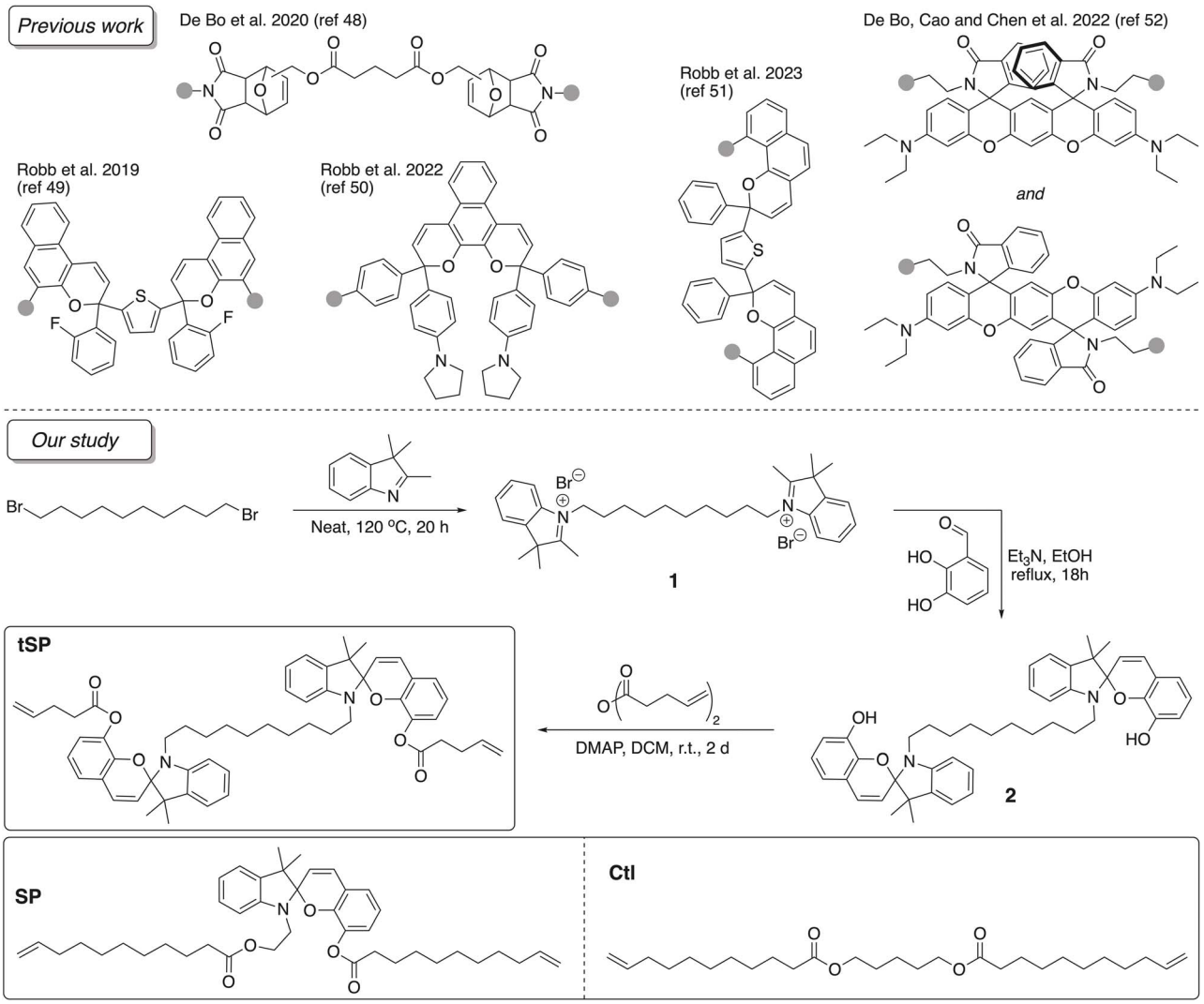

Scheme 1 Top: structures of tethered or fused bis-mechanophores in previous studies. Bottom: schematic synthesis of a tethered bis-spiropyran mechanophore with a long alkyl tether, and a spiropyran diene and a control diene molecule used in our study.

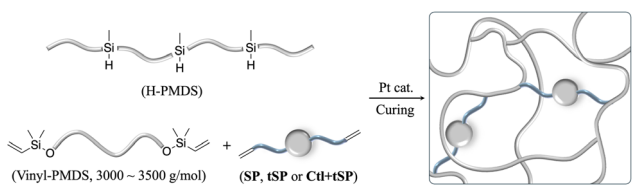

Fig. 2 Schematic incorporation of a mechanophore linker into PDMS elastomer networks using the commercial Sylgard 184 kit. The amount of added **SP**, **tSP** or **Ctl+tSP** diene is less than 2.2 mol% or 4.4 mol% relative to vinyl-PDMS.

not affected. Indeed, the resulting elastomer networks exhibited similar swelling ratios of 135–140% and gel fractions of 94–97% (Table S2†). The successful incorporation of the added diene linkers was verified by the characterization of the sol fraction using UV-vis spectroscopy, which revealed >92% incorporation of SP containing diene (Table S3†).

Table 1 Summary of the molar number and weight fraction of added linkers per gram of the PDMS elastomer network in the samples under study ($n = 5.8 \times 10^{-6}$ mol)

	N(SP)	N(tSP)	N(2SP)	N(Ctl+tSP)	N(2tSP)
tSP linker	—	n	—	n	$2n$
SP linker	n	—	$2n$	—	—
Ctl linker	—	—	—	n	—
Total wt%	0.38	0.5	0.76	0.76	1.0

Mechanophore activation under tensile testing

All samples were cut into a "dog bone" shape using an ISO 37 Type 4 cutting die (see the ESI† for details) and subjected to uniaxial tensile testing. Fig. 3 shows a representative set of images taken at various strains for the five samples of interest. All samples exhibited a clear blue colour at high strains, indicating the mechanical activation of SP mechanophores. The activation of SP at various strains was further quantified

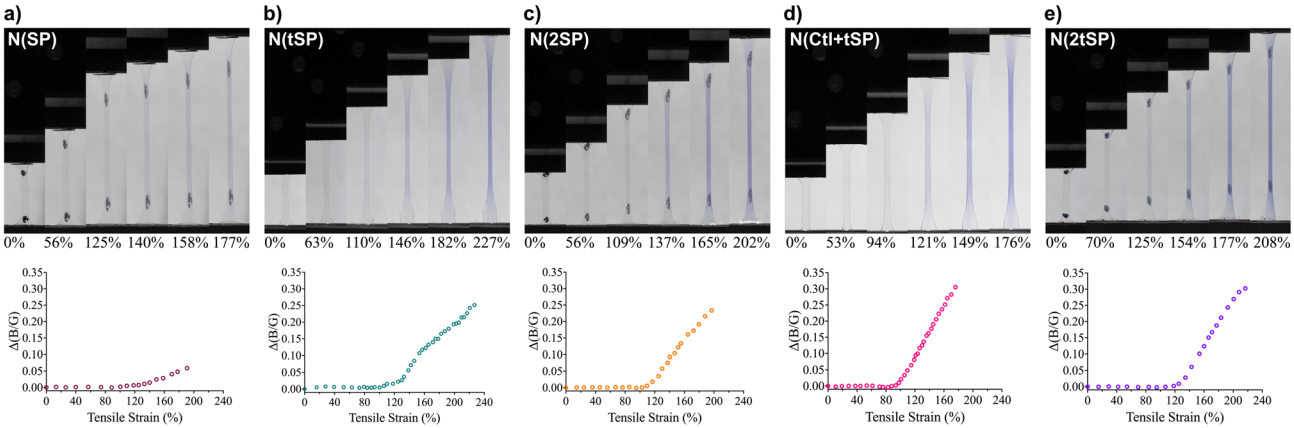

Fig. 3 Representative set of images and Δ(B/G) values of PDMS elastomer networks at various tensile strains. (a)–(e) Refer to **N(SP)**, **N(tSP)**, **N(2SP)**, **N(Ctl+tSP)**, and **N(2tSP)**, respectively. The images are calibrated using a standard grey card followed by an increase in exposure by 3 fold for the purpose of presentation, and the marked dots in (a), (c) and (e) were used to validate the tensile strain at the sample gauge sections. Images only present partial images acquired during the tensile tests, and each data point in the bottom graph indicates a Δ(B/G) value from image analysis at the corresponding strain.

through image analysis using B/G values. We plotted the increase in B/G value, denoted as Δ(B/G), as a function of strain. As shown in the plot of Δ(B/G) *vs.* tensile strain, Δ(B/G) remains near zero in the low-strain region (<100%), where entropic extension of polymer chains dominates. The activation of the SP mechanophore, indicated by an increase in Δ(B/G), occurs after 100% strain. Beyond this activation onset, the relative activation grows linearly. Previously, this specific SP mechanophore derivative was quantified by SMFS to activate at 415 pN in nonpolar media.[32] Polymer chains, such as PDMS chains,[57] experience such high force typically at strains corresponding to the enthalpic deformation of chains/bonds. Therefore, the activation of the SP mechanophore was typically observed to take place in the post strain-hardening region, and the onset of activation corresponds to the strain-hardening point, as has also been observed previously.[31,54,56]

We sought to compare the relative activation of these five samples by normalizing strain to the strain-hardening point. The stress–strain curves obtained from the tensile test are reasonably consistent for all samples (Fig. S4†), and the variance may have several origins, including (1) an error in thickness measurement of thin film samples (0.1–0.4 mm); (2) the "snapping" nature of the PDMS elastomer, which is closely related to propagating cracks primarily initiated by defects such as dust particles and voids in the film; and (3) pulling of materials out of the clamp during the tensile test. Determination of the strain-hardening point by identifying the intersection of linear fits to stress–strain curves before and after the nonlinear transition[54] seemed to be inconvenient and somewhat inconsistent in our experience. Fortunately, the intrinsic mechanical response of the SP mechanophore occurs at the strain-hardening point, enabling us to take the activation onset as the strain hardening point for normalization. An overlay of Δ(B/G) *vs.* normalized strain for four samples is shown in Fig. 4, and the relative activation post activation onset follows the order **N(2tSP)** > **N(Ctl+tSP)** > **N(2SP)** > **N(tSP)** > **N(SP)**.

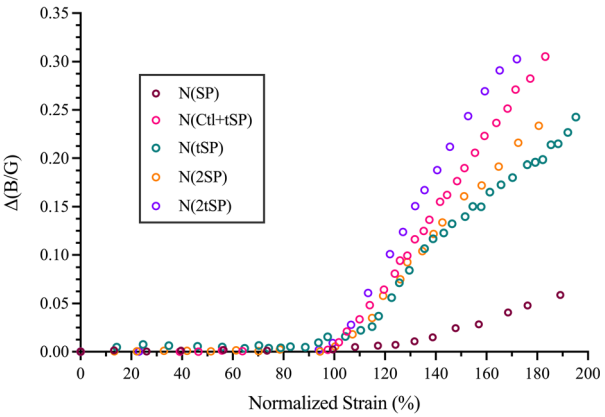

Fig. 4 Overlay of the representative set of Δ(B/G) values for the samples under study. The strain was normalized to the activation onset strain.

Material mechano-sensitivity and insights

The increase in Δ(B/G) with strain quantifies material mechano-sensitivity (SP activation per unit stain). Diverging trends observed after the activation onset reveals inherent differences in material mechano-sensitivity across the five samples.

To minimize potential human error and to provide insights into SP activation within PDMS elastomer networks, we reproduced the quantification studies and overlaid all data to evaluate systematic consistency. As shown in Fig. 5, the collected data from each sample clustered with acceptable variation. We further calculated the slope values of Δ(B/G) *versus* strain after the activation onset to quantify the material mechano-sensitivity. The grey areas indicate the variation range of slope values.

Table 2 summarizes the slope values for all five samples. Compared with **N(SP)**, the enhanced SP activation in **N(tSP)** is evident and significant. If we use the slope value to evaluate

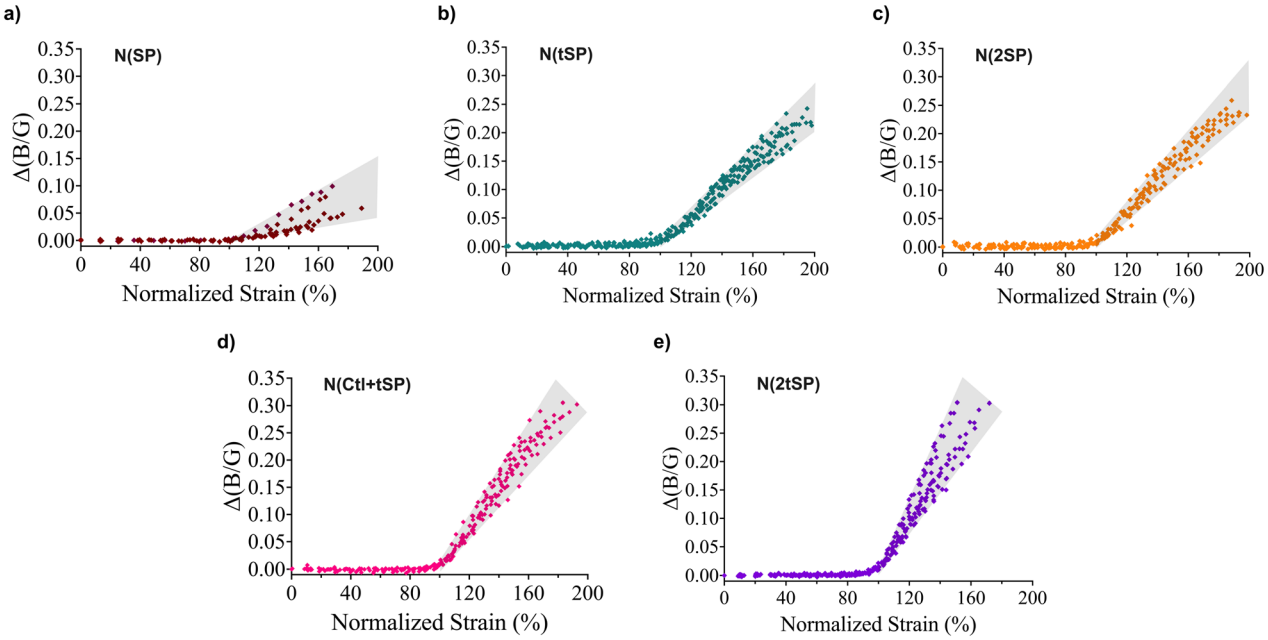

Fig. 5 Compiled plot of Δ(B/G) against normalized strain for all samples. (a) N(SP), (b) N(tSP), (c) N(2SP), (d) N(Ctl+tSP), and (e) N(2tSP). The strain was normalized to the activation onset, and the range of slope values is indicated by the grey area.

Table 2 Summary of the slope values of Δ(B/G) *vs.* normalized strain post the activation onset, or mechano-sensitivity of materials

N(SP)	N(tSP)	N(2SP)	N(Ctl+tSP)	N(2tSP)
0.10 ± 0.06	0.26 ± 0.03	0.30 ± 0.04	0.38 ± 0.07	0.49 ± 0.13

relative activation, the SP activation in **N(tSP)** is more than twofold higher than that in **N(SP)** (0.26 ± 0.03 *vs.* 0.10 ± 0.06), despite containing only twice the number of SP mechanophores. When doubling the number of **SP** linkers (denoted as sample **N(2SP)**), the slope value increases to 0.30 ± 0.04 (a near threefold increase). While a twofold increase in mechanophore linkers might theoretically double tension-bearing crosslinkers, the observed threefold activation enhancement suggests additional stress localization effects. This implies that increasing the number of these shorter mechanophore linkers (compared with the PDMS strands with an average molecular weight of 3000–3500 g mol^{-1} (ref. 57)) enables more tension to be concentrated on these short linkers. This effect is further supported by comparing **N(tSP)** and **N(Ctl+tSP)**. Though both contain identical **tSP** mechanophore quantities, **N(Ctl+tSP)** includes twice as many added linkers. Its substantially higher slope value (0.38 ± 0.07 *vs.* 0.26 ± 0.04) indicates that additional control linkers redistribute tension to a greater proportion of **tSP** mechanophores.

For **N(tSP)** and **N(2SP)**, both contain the same number of SP motifs; however, the number of added linkers in **N(2SP)** is twice that of **N(tSP)**. The effect of tension constraint, as mentioned earlier, likely contributes to the slightly higher activation observed in **N(2SP)** compared to **N(tSP)** (0.30 ± 0.04 *vs.* 0.26 ± 0.04). When the number of **tSP** linkers is increased to match the linker count in **N(2SP)**—as in **N(2tSP)**—the activation increases significantly from 0.26 ± 0.04 to 0.49 ± 0.13. If we assume a similar enhancement of SP activation for **N(2tSP)** as observed for **N(2SP)** relative to **N(SP)**, the expected activation would be approximately $0.26 \times 3 = 0.78$. However, the observed lower activation in **N(2tSP)** could be due to the aggregation of **tSP** linkers during material fabrication (Fig. S2†), resulting in heterogeneous incorporation of the **tSP** linker. In contrast, a homogeneous mixture indicating good dispersion and incorporation of both **Ctl** and **tSP** linkers was observed during the fabrication of **N(Ctl+tSP)** (Fig. S1†). If the **Ctl** linkers in **N(Ctl+tSP)** were replaced with **tSP** linkers, the calculated activation for **N(2tSP)** would be $0.38 \times 2 = 0.76$, aligning well with the expected enhancement in activation. Alternatively, we further prepared **N(Ctl+SP)** and observed a slope value of 0.16 ± 0.04 post the activation onset (Fig. S10†). Therefore, when comparing **N(Ctl+tSP)** and **N(Ctl+SP)** (0.38 ± 0.07 *vs.* 0.16 ± 0.04), this tethering design demonstrated a similar activation enhancement greater than twofold.

Amplification of mechanophore activation *via* a tethered design

From the comparison of **N(SP)** *vs.* **N(tSP)** and **N(Ctrl+SP)** *vs.* **N(Ctl+tSP)**, the tethering strategy appears to yield an amplification factor greater than two in SP activation. This enhancement is plausible, as the tethered design could facilitate simultaneous activation of two SP units under tension. Notably, simply doubling the **SP** linker—sample **N(2SP)**—instead of using the **tSP** linker appears to achieve a similar effect in this system. However, in polymer network systems where a SP mechanophore is used as the sole or main crosslinker,[58,59] doubling the number of crosslinkers would significantly alter the mechanical properties.

Conclusions

We have successfully demonstrated the amplification of SP mechanophore activation in bulk materials through a tethering strategy, with the enhancement observed to be slightly above twofold. This tethering strategy is reminiscent of the multi-mechanophore approach used for amplified mechanophore activation in ultrasonication studies of linear polymer solution.[60] Similar concepts involve effectively utilizing tension along the same polymer strand to activate multiple mechanophores rather than just one. Consequently, it is conceivable to explore designs incorporating more than two mechanophores in the linker for further activation enhancement in bulk materials. However, tethering too many mechanophores may result in the formation of long polymer chains that experience less tension within a polymer network under typical non-affine deformation. In contrast, tethering multiple mechanophores within a linear polymer chain for bulk studies offers significant activation enhancement, as recently demonstrated by Chen and workers.[61] They incorporated a rhodamine-rich polymer block into poly(methyl acrylate) and polyurethane matrices, achieving an activation enhancement by a factor of two. Lastly, our tethering strategy presented here can be adapted to other polymer network systems. We found that increasing the incorporation amount of mechanophore linkers results in greater tension constraints on these linkers. However, the poor compatibility of the **tSP** linker with the PDMS matrix limits further amplification through increased linker incorporation. We reason that incorporating additional mechanophore linkers would be more suitable for other polymer networks, such as polyacrylates, polyurethanes and gel systems.

Data availability

The data presented in this study are available on request from the corresponding author. Some data supporting this article have been included in the ESI.†

Author contributions

Y. L. conceived the project. Y. L. and S. N. designed the experiments. S. N. performed the syntheses, tensile test and image analysis. Z. Z. conducted the structural characterization of the small molecules. S. N., Z. Z. and Y. L. discussed the results. Y. L. wrote the manuscript.

Conflicts of interest

There are no conflicts to declare.

Acknowledgements

The work performed in this study was supported by a startup grant offered by the Chemistry Department at the University of Waterloo and by the funding from the Natural Sciences and Engineering Research Council of Canada (NSERC). We also acknowledge the support of the NMR Facility and the Mass Spectrometry Facility in the Chemistry Department at the University of Waterloo.

References

1 K. S. R. Chandran, *Polymer*, 2016, **91**, 222–238.
2 S. A. R. Naga and T. A. El-Sayed, *Journal of Failure Analysis and Prevention*, 2024, **24**, 922–935.
3 H. Staudinger, *Berichte der deutschen chemischen Gesellschaft (A and B Series)*, 1930, **63**, 921–934.
4 T. Sato and D. E. Nalepa, *J. Appl. Polym. Sci.*, 1978, **22**, 865–867.
5 S. L. Malhotra, *J. Macromol. Sci., Part A*, 1986, **23**, 729–748.
6 T. Andersson, B. Wesslén and J. Sandström, *J. Appl. Polym. Sci.*, 2002, **86**, 1580–1586.
7 M. V. Encina, E. Lissi, M. Sarasúa, L. Gargallo and D. Radic, *J. Polym. Sci., Polym. Lett. Ed.*, 1980, **18**, 757–760.
8 K. L. Berkowski, S. L. Potisek, C. R. Hickenboth and J. S. Moore, *Macromolecules*, 2005, **38**, 8975–8978.
9 D. A. Davis, A. Hamilton, J. Yang, L. D. Cremar, D. Van Gough, S. L. Potisek, M. T. Ong, P. V. Braun, T. J. Martínez, S. R. White, J. S. Moore and N. R. Sottos, *Nature*, 2009, **459**, 68–72.
10 J. Li, C. Nagamani and J. S. Moore, *Acc. Chem. Res.*, 2015, **48**, 2181–2190.
11 I. M. Klein, C. C. Husic, D. P. Kovács, N. J. Choquette and M. J. Robb, *J. Am. Chem. Soc.*, 2020, **142**, 16364–16381.
12 R. T. O'Neill and R. Boulatov, *Nat. Rev. Chem.*, 2021, **5**, 148–167.
13 Y. Chen, G. Mellot, D. van Luijk, C. Creton and R. P. Sijbesma, *Chem. Soc. Rev.*, 2021, **50**, 4100–4140.
14 B. A. Versaw, T. Zeng, X. Hu and M. J. Robb, *J. Am. Chem. Soc.*, 2021, **143**, 21461–21473.
15 R. Küng, R. Göstl and B. M. Schmidt, *Chem.–Eur. J.*, 2022, **28**, e202103860.
16 R. Groote, R. T. M. Jakobs and R. P. Sijbesma, *Polym. Chem.*, 2013, **4**, 4846–4859.
17 Y. Yu, R. T. O'Neill, R. Boulatov, R. A. Widenhoefer and S. L. Craig, *Nat. Commun.*, 2023, **14**, 5074.
18 Y. Zhao, X. Guo, F. Gao, C. Fu, L. Shen and J. Ma, *Eur. Polym. J.*, 2024, **218**, 113360.
19 X. Liang and H. Qian, *Chin. J. Chem.*, 2025, **43**, 349–354.
20 Y. Chen, G. Sanoja and C. Creton, *Chem. Sci.*, 2021, **12**, 11098–11108.
21 A. Cartier, O. Taisne, S. Ivanov, J. Caillard, M. Couty, J. Comtet and C. Creton, *Macromolecules*, 2024, **57**, 8712–8721.
22 T. A. Kim, C. Lamuta, H. Kim, C. Leal and N. R. Sottos, *Advanced Science*, 2020, **7**, 1903464.
23 J. A. Gohl, T. J. Roberts, A. C. Freund, N. Haque, L. M. Rueschhoff, L. A. Baldwin and C. S. Davis, *RSC Mechanochem.*, 2025, **2**, 178–183.
24 Y. Chen, C. J. Yeh, Y. Qi, R. Long and C. Creton, *Sci. Adv.*, 2020, **6**, eaaz5093.
25 G. E. Sanoja, X. P. Morelle, J. Comtet, C. J. Yeh, M. Ciccotti and C. Creton, *Sci. Adv.*, 2021, **7**, eabg9410.

26 R. T. O'Neill and R. Boulatov, *Angew. Chem., Int. Ed.*, 2024, **63**, e202402442.
27 K. Zheng, Y. Zhang, B. Li and S. Granick, *Nat. Commun.*, 2023, **14**, 537.
28 Y. Huang, S. Huang and Q. Li, *ChemPlusChem*, 2023, **88**, e202300213.
29 M. Li, Q. Zhang, Y.-N. Zhou and S. Zhu, *Prog. Polym. Sci.*, 2018, **79**, 26–39.
30 M. Sommer, *Macromol. Rapid Commun.*, 2021, **42**, 2000597.
31 Y. Lin, M. H. Barbee, C.-C. Chang and S. L. Craig, *J. Am. Chem. Soc.*, 2018, **140**, 15969–15975.
32 Y. Lin, T. B. Kouznetsova, A. G. Foret and S. L. Craig, *J. Am. Chem. Soc.*, 2024, **146**, 3920–3925.
33 Q. Mu and J. Hu, *Phys. Chem. Chem. Phys.*, 2024, **26**, 679–694.
34 R. Adhikari and D. E. Makarov, *J. Phys. Chem. B*, 2017, **121**, 2359–2365.
35 G. R. Gossweiler, T. B. Kouznetsova and S. L. Craig, *J. Am. Chem. Soc.*, 2015, **137**, 6148–6151.
36 Y. Lin, T. B. Kouznetsova and S. L. Craig, *J. Am. Chem. Soc.*, 2020, **142**, 99–103.
37 T. A. Kim, B. A. Beiermann, S. R. White and N. R. Sottos, *ACS Macro Lett.*, 2016, **5**, 1312–1316.
38 B. A. Beiermann, S. L. B. Kramer, J. S. Moore, S. R. White and N. R. Sottos, *ACS Macro Lett.*, 2012, **1**, 163–166.
39 C. Wang, S. Akbulatov, Q. Chen, Y. Tian, C.-L. Sun, M. Couty and R. Boulatov, *Nat. Commun.*, 2022, **13**, 3154.
40 J. M. Lenhardt, A. L. Black, B. A. Beiermann, B. D. Steinberg, F. Rahman, T. Samborski, J. Elsakr, J. S. Moore, N. R. Sottos and S. L. Craig, *J. Mater. Chem.*, 2011, **21**, 8454–8459.
41 J. Noh, G. I. Peterson and T.-L. Choi, *Angew. Chem., Int. Ed.*, 2021, **60**, 18651–18659.
42 T. Watabe, D. Aoki and H. Otsuka, *Macromolecules*, 2021, **54**, 1725–1731.
43 D. W. Kim, G. A. Medvedev, J. M. Caruthers, J. Y. Jo, Y.-Y. Won and J. Kim, *Macromolecules*, 2020, **53**, 7954–7961.
44 H. Zhang, D. Zeng, Y. Pan, Y. Chen, Y. Ruan, Y. Xu, R. Boulatov, C. Creton and W. Weng, *Chem. Sci.*, 2019, **10**, 8367–8373.
45 W. Qiu, P. A. Gurr and G. G. Qiao, *Macromolecules*, 2020, **53**, 4090–4098.
46 Q. Sheng, R. Tan, X. Zhang, H. Shen and Z. Zhang, *ACS Macro Lett.*, 2024, **13**, 1670–1677.
47 Y. Liao, B. Le Roi, H. Zhang, C. E. Diesendruck and J. M. Grolman, *J. Am. Chem. Soc.*, 2024, **146**, 17878–17886.
48 R. Stevenson, M. Zhang and G. De Bo, *Polym. Chem.*, 2020, **11**, 2864–2868.
49 M. E. McFadden and M. J. Robb, *J. Am. Chem. Soc.*, 2019, **141**, 11388–11392.
50 M. E. McFadden, S. K. Osler, Y. Sun and M. J. Robb, *J. Am. Chem. Soc.*, 2022, **144**, 22391–22396.
51 S. K. Osler, M. E. McFadden, T. Zeng and M. J. Robb, *Polym. Chem.*, 2023, **14**, 2717–2723.
52 M. Wu, Y. Li, W. Yuan, G. De Bo, Y. Cao and Y. Chen, *J. Am. Chem. Soc.*, 2022, **144**, 17120–17128.
53 G. R. Gossweiler, G. B. Hewage, G. Soriano, Q. Wang, G. W. Welshofer, X. Zhao and S. L. Craig, *ACS Macro Lett.*, 2014, **3**, 216–219.
54 T. Ouchi, W. Wang, B. E. Silverstein, J. A. Johnson and S. L. Craig, *Polym. Chem.*, 2023, **14**, 1646–1655.
55 M. J. Robb, T. A. Kim, A. J. Halmes, S. R. White, N. R. Sottos and J. S. Moore, *J. Am. Chem. Soc.*, 2016, **138**, 12328–12331.
56 T. A. Kim, M. J. Robb, J. S. Moore, S. R. White and N. R. Sottos, *Macromolecules*, 2018, **51**, 9177–9183.
57 S. Lu, W. Cai, N. Cao, H.-j. Qian, Z.-y. Lu and S. Cui, *ACS Mater. Lett.*, 2022, **4**, 329–335.
58 C. M. Kingsbury, P. A. May, D. A. Davis, S. R. White, J. S. Moore and N. R. Sottos, *J. Mater. Chem.*, 2011, **21**, 8381–8388.
59 C. K. Lee, C. E. Diesendruck, E. Lu, A. N. Pickett, P. A. May, J. S. Moore and P. V. Braun, *Macromolecules*, 2014, **47**, 2690–2694.
60 B. H. Bowser and S. L. Craig, *Polym. Chem.*, 2019, **10**, 6523.
61 S. Zhang, Y. Gao, Y. Wang, M. Wu, X. Huang, Z. Wu, J. Wang, Y. Chen and Y. Yuan, *Macromolecules*, 2025, **58**, 2259–2265.